

2016-02-10

# Acellular Reactivity of Polymeric Dendrimer Nanoparticles as an Indicator of Oxidative Stress in Vitro

Marcus Maher
*Technological University Dublin*, Marcus.Maher@mydit.ie

Humza Khalid
*Technological University Dublin*

Hugh Byrne
*Technological University Dublin*, hugh.byrne@tudublin.ie



## Recommended Citation

Byrne, H.J., Maher, M. A., & Khalid, H. (2016) Acellular reactivity of polymeric dendrimer nanoparticles as an indicator of oxidative stress in vitro", *Analytical and Bioanalytical Chemistry,* 408, 695-703 (2016). doi:10.1007/s00216-015-9171-7

**Acellular reactivity of polymeric dendrimer nanoparticles as an indicator of oxidative stress *in vitro*.**

Marcus A. Maher[1,2,†], Humza Khalid[1,2,†], Hugh J. Byrne[1]*

[1] FOCAS Research Institute, Dublin Institute of Technology, Kevin Street, Dublin 8, Ireland,

[2] School of Physics, Dublin Institute of Technology, Kevin Street, Dublin 8, Ireland,

[†]Equal First Author

*Corresponding Author: Hugh.Byrne@DIT.IE

## Abstract

The need for rapid and cost effective pre-screening protocols of the toxicological response of the vast array of emerging nanoparticle types is apparent and the emerging consensus on the paradigm of oxidative stress by generation of intracellular reactive oxygen species as a primary source of the toxic response suggests the development of acellular assays to screen for nanoparticle surface reactivity. This study explores the potential of the monoamine oxidase A (MAO-A) enzyme based assay with polymeric dendrimers as cofactors and serotonin as substrate, which generates $H_2O_2$, quantified by the conversion of the Carboxy-$H_2$DCFDA dye to its fluorescent form. A range of generations of both PAMAM (poly(amido amine)) (G4-G7) and PPI (poly(propylene imine)) (G0-G4) dendritic polymer nanoparticles are used as test particles to validate the

quantitative nature of the assay response as a function of nanoparticle physico-chemical properties. The assay is well behaved as a function of dose, over low dose ranges and the acellular reaction rate (ARR) is well correlated with the number of surface amino groups for the combined dendrimer series. For each series, the ARR is also well correlated with the previously documented cytotoxicity, although the correlation is substantially different for each series of dendrimers, pointing to the additional importance of cellular uptake rates in the determination of toxicity.

**Abbreviations used:** MAO-A: Monoamine Oxidase A, $H_2O_2$: Hydrogen Peroxide, PAMAM: Poly(amido-amine), PPI: Poly(propylene-imine), G: generation, ARR: Acellular Reaction Rate.

**Keywords:** Nanotoxicity, dendrimer nanoparticles, oxidative stress, acellular assay.

## Introduction

Nanoparticle science has seen a surge of interest in recent years which continues to increase. Already there are over 1600 listed products and technologies which in some way utilise nanoscience in the areas of: electronics, engineering, cosmetics, food, textiles, packaging and many more.[1] However the use of nanoparticles in the fields of medicine and drug delivery continue to be of particular importance.[2] It is known that nanoparticles have the ability to enter into mammalian cells, and while this has many potential medical applications, it also initiates a toxic response which can lead to cell death.[3] Therefore, it is important to evaluate the toxic potential of nanoparticles.

Currently, the first step in evaluating toxicity is the use of *in vitro* cytotoxicity assays such as: Alamar Blue (AB), Neutral Red (NR) and 3-(4,5-dimethylthiazol-2-yl)-2,5-diphenyltetrazolium bromide (MTT).[4] These assays are both time consuming and relatively costly in terms of their application and optimisation. It is becoming apparent, that to keep up with the immense range of emerging nanoparticles, efforts must be made to both increase the efficiency of current methods and to develop alternative methods to rapidly screen nanoparticles for toxic potential.[4,5,6,7]

One way to aid in this endeavour is the development of predictive models for toxicity. These models can be guided by, or identify, Adverse Outcome Pathways (AOPs), a systematic sequence of causally linked events which leads to an adverse health (or ecotoxicological) outcome.[8] However, our current understanding of nanoparticle toxicity at the cellular level is lacking, therefore such models require an extensive amount of screening and analysis of nanoparticle toxic responses and mechanisms, ultimately using *in vitro* and *in vivo* methods.[9,10] Modelling efforts can also be aided by

quantitative structure activity relationships (QSARs), which extend the use of the existing knowledge by correlating adverse outcomes with physico-chemical characteristics, which can ultimately guide synthetic strategies.[11]

The report of the EU Nanosafety Cluster, Working Group 10 has advocated a hierarchical, concern driven approach to nanoparticle testing, in which tier 1 is based on physico-chemical properties and for example structure–activity relationships. [5] Oxidative stress has been identified as one of the initial adverse system responses giving rise to nanoparticle toxicity *in vitro*,[12] and this is most prominent in nanoparticles with cationic effective surface charges, such as aminated nanoparticles.[13] It can be argued, therefore, that to develop a protocol for determination of nanoparticle surface reactivity would be an invaluable first tier procedure in a hierarchical nanotoxicology screening strategy. Such a pre-screening approach could aid in the optimisation of current *in vitro* methods, thereby reducing the overall time needed for the initial screening process.

For the development and validation of such an assay, it is important to use a set of structurally well defined nanoparticles. In this study, PAMAM (poly(amido amine)) and PPI (poly(propylene imine)) dendritic polymer nanoparticles are used, as they have the required well defined structures and have been shown to produce systematically variable toxic responses in mammalian cells[10,14,15,16] and in a battery of eco-toxicological assays.[17,18] These particles are created via the addition of branches onto a core molecule, whereby the addition of each set of branches results in successive dendrimer generations. The added branches each have two terminal groups which can be used for the addition of further branches, so that the number of termini increases with increasing generation.(*Images available at: symo-chem.nl, 2015 & dendritech.com, 2015*)[19,20]

These termini can then be modified to be cationic, anionic or neutral. Studies show that cationic nanoparticles can enter into human cells and initiate a toxic response more readily than their anionic or neutral counterparts.[21] Therefore, amine modified PPI and PAMAM nanoparticles are used here. Both PAMAM and PPI dendrimers have several potential applications, including: drug delivery agents,[22, 23] gene delivery agents,[24, 25] exploring and altering cellular signalling pathways [26] and to probe cellular uptake mechanisms.[27] PAMAM and PPI dendrimers are in the lower range of the definition of a nanoparticle (1nm – 100nm) (*EC: 2011/696/EU*).[28] PAMAMs used in this study have sizes (as determined by AFM): 2.1-2.8nm (G4), 4.1-4.6nm (G5), 4.2 – 5.8nm (G6) [27] and G7 ≈ 8.1nm (G7 theoretical diameter determined by: *Dendritech, 2015*[20]). PPI sizes (as determined by AFM) are: ≈1.23nm (G0), ≈1.8nm (G1), 1.7 – 1.9nm (G2), 1.8 – 2.6nm (G3) and 2.5 – 3.5nm (G4).[27] The lower generation PPI are at the extreme of the nanoparticle definition and have been used to probe the interface where active cellular uptake gives way to passive diffusion,[27] and therefore a definition of "nano-scale macromolecules" may be more appropriate for these species. However, for the purpose of this study, they make excellent model particles due to the aforementioned systematically variable physico-chemical properties.

Reactive Oxygen Species (ROS) generation, upon dendrimer endocytosis, has been identified as the initial step in the toxic response[15,16,27] and, in the case of cationic nanoparticles in the acidifying environment of endosomes, it is reported that the unsaturated surface amino groups sequester protons that are supplied by the v-ATPase (proton pump) and may be mediated via NADPH oxidase activity.[29] The generation of ROS is counteracted by the natural intracellular antioxidant processes, although the ROS

generation can dominate, leading to oxidative stress and ultimately apoptosis via subsequent mitochondrial damage.[15] A number of studies have demonstrated that the response is systematically dependent on the number of surface amino groups[10,14,15,16,27] and *Maher et al.(2014)* have modelled the uptake and intracellular responses, leading to apoptosis, using a rate equation model.[9] The rate of generation of ROS is dependant on the number of surface amino groups on the nanoparticle and this also governs the surface reactivity. Therefore, the *in vitro* toxicity is intrinsically linked with the surface reactivity of the nanoparticles, which, it is proposed, can be measured acellularly. Acellular based assay systems have previously been used to assess the surface reactivity of nanoparticles.[30]

In this work, the Monoamine Oxidase A (MAO-A) enzyme is employed to probe the acellular production of ROS by homologous series of polymeric dendrimer nanoparticles. The use of the two related, homologous dendrimer series, PAMAM and PPI, enables an evaluation of the ability of the assay to not only register surface activity, but also to quantify the activity in relation to the systematically varied dendrimer structure. Attempts can then be made to correlate the acellular reactivity with the cellular cytotoxicity as previously measured using established cytotoxicity assays. The study is a route towards establishing a time efficient alternative method for the analysis of nanoparticle toxicity and may also aid predictive modelling based on structure activity relationships.

## Materials and Methods

### Materials

Serotonin hydrochloride, Horseradish peroxidise (HRP), Monoamine Oxidase-A (MAO-A)FAD-bound (E.C:1.4.3.4) were purchased form Sigma-Aldrich. The Poly(amidoamine) nanoparticles (PAMAM) generations 4-7, were purchased from Sigma-Aldrich and manufactured by Dendritech Inc. The poly(propyl imine) (PPI) dendrimers generation 0-4, were purchased from SyMO-Chem. The Carboxy-$H_2$DCFDA was purchased from Invitrogen. The 96 well plates used were purchased from TrueLine and all plates were analysed in a Molecular Devices SpectraMax M3 spectrometer.

### Methodology

Enzymatic reaction

An enzymatic approached was taken using Monoamine Oxidase-A (MAO-A), a flavin-containing amine oxidoreductase, which catalyses the oxidative deamination of its substrate, producing an aldehyde and an amine, as shown in Figure 1. Hydrogen peroxide ($H_2O_2$) is produced as a by-product. In this study, the substrate chosen was serotonin, which is converted to 5-hydroxyindole acetaldehyde with the release of ammonia ($NH_3$) and hydrogen peroxide ($H_2O_2$). The production of hydrogen peroxide can be easily detected with the dye: 6-carboxy-2',7'-dichlorodihydrofluorescein diacetate (Carboxy-$H_2$DCFDA), a fluorescein derivative, which is converted to its fluorescent form via the cleavage of its acetate groups and oxidation by ROS.

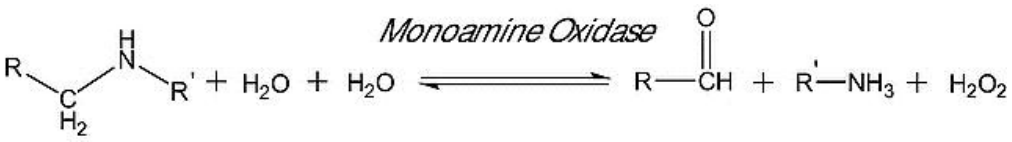


Figure 1: Generalised reaction mechanism of Monoamine Oxidase-A In the case of this study, serotonin was used as a substrate (therefore R' is H) and the products are 5-hydroxyindole acetaldehyde, hydrogen peroxide ($H_2O_2$) and ammonia ($NH_3$).[31]

The reaction was carried out in PBS, which ensured that more than enough water was present to allow the amount of serotonin to be the limiting factor in the reaction. It is proposed that, in the presence of aminated nanoparticles, the production of $H_2O_2$ (via enzymatic action) is further promoted and thus can be used to measure the surface reactivity.[32,33,34]

Surface Amine Calculation

For both dendrimer series, the number of surface amino groups can be calculated via the formula:

$$N_{amg} = N_{BP(G0)}.2^{G} \qquad \text{Equation 1}$$

-where $N_{amg}$ is the number of surface amino groups, $N_{BP(G0)}$ is the number of initial binding sites on the core of the particle (for PAMAM and PPI dendrimers: $N_{BP(G0)}$=4), and *G* is the generation of the nanoparticle.[9]

Experimental Procedure

An 800μM solution of Serotonin was made up in Phosphate Buffer Solution (PBS). PAMAM or PPI nanoparticles were made up in this solution. The concentration range

used for PAMAM was: 0.08-5.2μM for all generations (G4, G5, G6 and G7). The concentration ranges used for PPI were: G0: 25-3500μM, G1: 5-3000μM, G2: 5-35μM, G3: 0.325-3.5μM, and G4: 0.6-3.0μM. The concentration ranges were chosen to encompass and span the effective concentration for 50% loss of viability ($EC_{50}$) in the immortal keratinocyte (HaCaT) cell line for each particle, as determined by the 3-(4,5-dimethylthiazol-2-yl)-2,5-diphenyltetrazolium bromide (MTT) assay.[14,15,16,27] 100μL of each concentration was added to the 96-well plate. Six replicates of each concentration were made on the plate and the enzyme MAO-A (concentration: 0.0075mg/mL) was added to the first 3 wells of each concentration (the second 3 wells contained no enzyme and were used as a control -see supplementary material for a more detailed explanation of experimental setup). The plate was then left at 37˚C for 10 minutes to allow the MAO-A to act on the serotonin and produce ROS. After 10 minutes incubation, 100μL of the Carboxy-$H_2$DCFDA dye (containing 2.2U/mL HRP to enhance fluorescence)[35] was added to the wells to a final concentration of 10μM and this was again left at 37˚C for 10 minutes to allow for colour development. The plates were then read using a Molecular Devices SpectraMax M3 spectrometer with: $\lambda_{ex}$ = 488nm and $\lambda_{em}$= 535nm.

SigmaPlot™ (v.10.0) was used for all data analysis and generation of graphs; all error bars are ± standard deviation. Each plate contained three replicates of each concentration and each plate was repeated three times. Numerical simulations were performed by integration using the iterative Euler approach and again SigmaPlot™ (v.10.0) was used to generate the values and graphs.

## Results

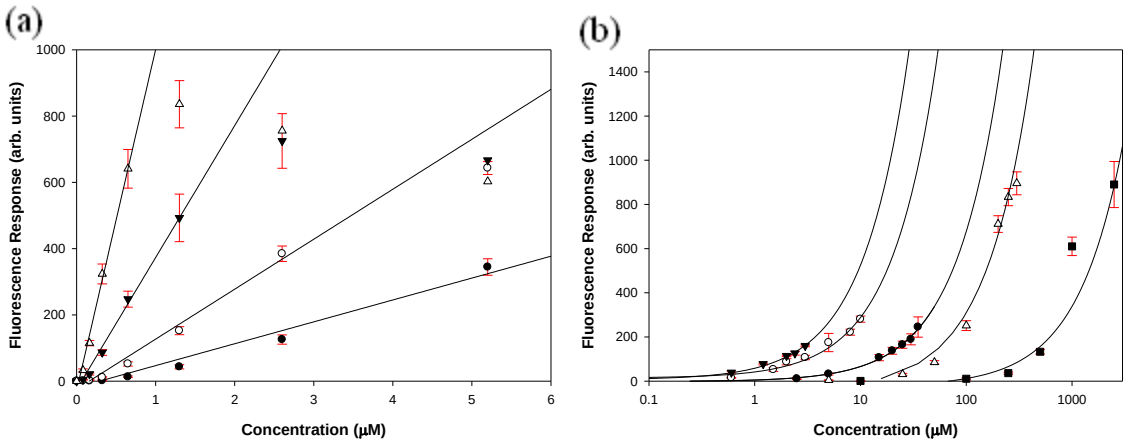


Figure 2 (a): Plot of the concentration dependent fluorescence intensity for PAMAM dendrimers G4(●), G5(○), G6(▼), G7(Δ) (b): Plot of the concentration dependent fluorescence intensity for PPI dendrimers G0(■), G1(Δ), G2(●), G3(○) , G4 (▼). The lines are a linear regression fit to the data.

Figure 2a shows the concentration dependence of the fluorescence generated by the PAMAM dendrimer nanoparticles over the concentration range 0.08 – 5.2μM for generations G4 - G7. In this experimental setup, the increasing fluorescence is a result of increasing dose and generation of ROS and their interaction with the dye (Carboxy-$H_2$DCFDA). Figure 2b shows the similar concentration dependence of the fluorescence generated by the PPI dendrimer nanoparticles over the concentration range 0-3500μM for generations G0 – G4. The extended range is necessary due to the reduced activity of the lower generation PPI dendrimers, and the data is shown in a semi-log plot for best visualisation of the full range of concentrations employed.

The fluorescence generation is dependent on the combined presence of the enzyme and the dendrimer (see supplementary material), the latter in a dose dependent fashion. Therefore, it is proposed that the increased $H_2O_2$ generation is analogous to a measurement of nanoparticle reactivity. This reactivity increases linearly over the initial concentration range tested, although deviation at the higher concentrations for higher dendrimer generations is observed. Regression to the lower concentration range produces a linear fit, the slope of which is a measure of the Acellular Reaction Rate (ARR) of the nanoparticles (solid lines in Figure 2).

(a) (b)

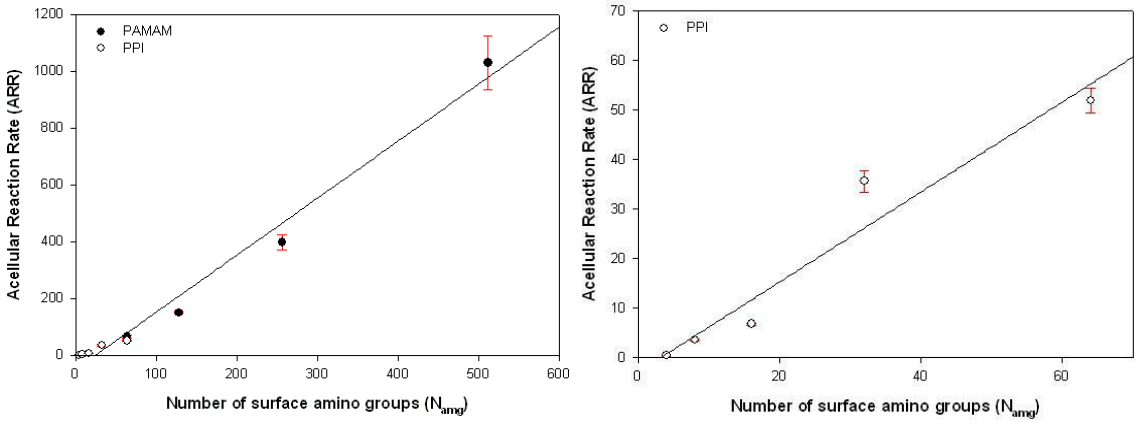


Figure 3: (a) Plot of the slope as a function of Number of Surface Amino Groups ($N_{amg}$) for all PAMAM and PPI dendrimers. The solid line shows a fit to a linear dependence for the combined dendrimer series. (b) Plot of the slope as a function of Number of Surface Amino Groups for PPI dendrimers. The solid line shows a fit to a linear dependence.

The concentration dependent fluorescence generation, indicative of the ROS response, elicited by PAMAM and PPI dendrimers, is not only concentration dependence but is clearly also generation dependent. For both homologous dendrimer series, increased

generation and therefore number of surface amino groups ($N_{amg}$) produces an increase of the ARR. Figure 3(a) shows a combined plot of the ARR for both PAMAM and PPI dendrimer series, versus $N_{amg}$ for progressive dendrimer generations, while Figure 3(b) focuses on the PPI response. The graph shows a clear correlation of ARR with $N_{amg}$ for both series. The generation dependence of the conversion of the dye to its fluorescent form is therefore clearly dependent on the surface properties of the dendrimer. Notably, the approximately linear trend is similar for the two dendrimer series, indicating that the ARR is determined by the surface amino groups, independent of the differences in core structure of the PAMAM and PPI dendrimers.

Critically, the *in vitro* cytotoxicity of both PAMAM and PPI dendrimers shows a similar dose and generation dependence[14,15,16,27] and it has been demonstrated that the initial stages of the cellular response are associated with oxidative stress in endosomes, upon endocytosis.[15] *Maher et al. (2014)* have demonstrated that this *in vitro* oxidative stress can be modelled according a rate equation system, in which the rate of ROS production is dependent on generation and therefore $N_{amg}$[9], prompting a comparison of the ARR with the measured cytotoxicity of the nanoparticles.

Figure 4a shows a plot of the acellular ROS activity against the cytotoxicity for both dendrimer series (Figure 4b for the PPI series alone), as previously determined in the HaCaT cell line using the MTT assay at 24hrs, represented by the inverse $EC_{50}$.[14,15,16] A good, approximately linear, correlation is observed between the two parameters, although the relationship is clearly different for each of the dendrimer series. The correlation within each individual series is a clear indication that the ARR is a

measure of the intracellular ROS generation, *in vitro*, which in turn is predictive of the *in vitro* cytotoxic response.

(a) (b)

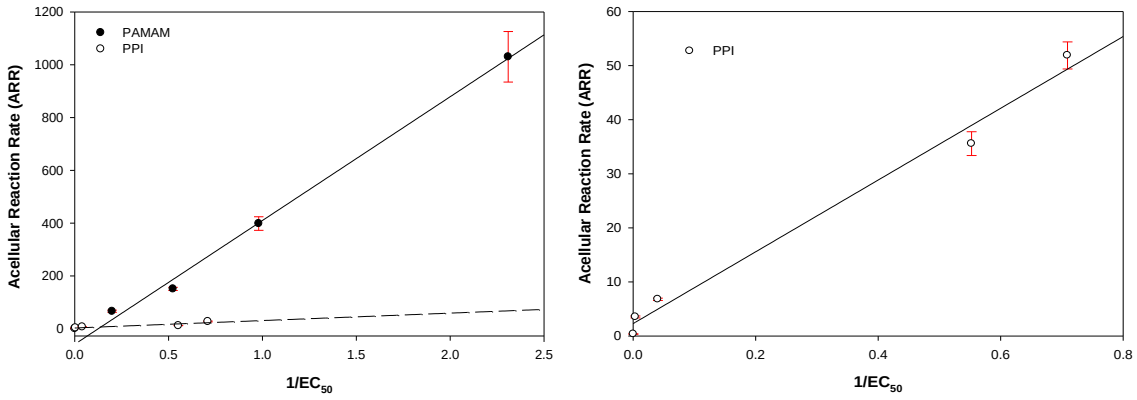


Figure 4 (a): Plot of the Acellular reaction rate (ARR) for all PAMAM and PPI dendrimers versus the inverse cytotoxicity as previously measured using the MTT assay.[14,15,16] (b): Plot of the Acellular reaction rate (ARR) for PPI dendrimers versus the inverse cytotoxicity as previously measured using the MTT assay. The lines show a fit of linear dependences.

Notably, however, the assay does not translate between the two related homologous series, indicating that it cannot be universally applied to all nanoparticles with apparently equivalent surface chemistry. The origin of the difference in the responses is explored further in the following section.

The error bars in Figure 4 are derived from those of the reported $EC_{50}$ values, which were obtained from previously published work [14,15,16] and are 95% Confidence Intervals derived from fitting the dose dependent viability to a sigmoidal curve and a four

parameter logistic model using Xlfit3$^{TM}$, a curve fitting add-on for Microsoft® Excel (*ID Business Solutions, UK*).

**Discussion**

Polymeric dendrimers are homologous series of nano-meter scale molecules with systematically variable cytotoxic responses, which have been shown to correlate with the precisely variable surface structure, in the case of PAMAM and PPI, the number of surface amino groups. Upon endocytosis, the initial stage of the cellular response has been demonstrated to be oxidative stress, which has also been seen to correlate well with the dendrimer generation and therefore number of surface amino groups.[14,15,16,27]

In a rate equation model of the cellular responses and cytotoxicity, the oxidative stress and subsequent inflammatory cascade and loss in viability, keeping all cellular parameters constants, it was demonstrated that variation of the single generation dependent parameter, representing surface reactivity, resulted in a faithful simulation of the range of responses for PAMAM G4-G6.[9] It can therefore be argued that measurement of this surface reactivity, acellularly, can serve as a predictor for the *in vitro* toxicity of the nanoparticles, with significant time, labour and cost savings.

Both homologous dendrimer series, PPI and PAMAM, showed a generation and concentration dependant conversion of serotonin and resultant generation of $H_2O_2$, as monitored by the fluorescent ROS assay, Carboxy-$H_2$DCFDA. The relationship between generated fluorescence and dendrimer dose was seen to be linear, at least over the lower dose range (Figures 2a and b) and the rate of increase as a function of dose can be considered representative of the rate of reactivity of the NPs in an acellular environment, or the Acellular Reaction Rate (ARR). In Figure 3, the ARR is seen to be approximately linearly dependant on the $N_{amg}$ (and therefore dendrimer generation) for both series,

independent of the core structure. Crucially, a similar relationship (between $N_{amg}$ and ROS) can be seen in various toxicological studies.[14,15,16,27]

The acellular assay used in this work exploits the conversion of the dye Carboxy-$H_2$DCFDA to its fluorescent form by interaction with the generated $H_2O_2$. The control reactions detailed in the supplementary information confirm that the measured fluorescence generation is dependent on the simultaneous presence of the enzyme and dendrimer. To confirm the role which the dendrimer nanoparticles play in the reaction, the system can be modelled with a rate equation system:

$$\frac{dN_{H2O2}}{dt} = (k_{ROS}.N_{sero}(t).N_{H2O}(t)) - (k_{enz}.k_{21}.N_{ald}(t).N_{ami}(t).N_{H2O2}(t)) - (k_{31}.N_{DCF}(t).N_{H2O2}(t)^n)$$

- Equation 2

where $N_{H2O2}$ denotes the number of $H_2O_2$ species generated, at a rate $k_{ROS}$, depending on the number of serotonin, $N_{sero}$, and water, $N_{H2O}$, molecules present. The rate is reduced by the reverse reaction of the product species $N_{ald}$ and $N_{ami}$, at a rate $k_{21}$, and by the interaction of the $H_2O_2$ species generated with the dye concentration, $N_{DCF,}$ to produce the fluorescent form of the dye $N_F$ at a rate $k_{31}$, according to the equation

$$\frac{dN_F}{dt} = (k_{31}.N_{DCF}(t).(N_{H2O2}(t)^n)) - (k_q.N_F(t).N_D(t)) \qquad \text{Equation 3}$$

The rate $k_{ROS}$ is determined by the dendrimer dose, $N_D$, and generation (represented by number of surface amino groups, $N_{amg}$), as well as the enzyme concentration, which determines the enzymatic reaction rate ($k_{ENZ}$), according to the equation:

$$k_{ROS} = (k_{ENZ}).(N_D).(A).(k_{12}) \qquad \text{Equation 4}$$

-where $k_{12}$ is a dose and generation independent rate constant, and

$A = N_{amg}(G+1)$

Figure 5 shows a simulation of the response for dendrimers of generation 3-7 (independent of dendrimer type). The parameter varied between the simulations for each dendrimer generation is $N_{amg}$. In the simulation, a value of the empirical factor $n=2$ for the interaction of the $H_2O_2$ with the Carboxy-$H_2$DCFDA dye is used, consistent with cleavage of two acetate groups by oxidation to produce the fluorescent form of the dye.[36] The simulated response faithfully reproduces the experimentally observed generation dependence across all generations. Notably, the reduction of fluorescence at higher doses for the higher order generations is best reproduced by a quenching of the fluorescence of the converted dye by interaction with the dendrimers, indicated by the second term of equation 3 at a rate $k_q$, rather than a fouling or consumption of the enzyme or dendrimers in the primary reaction of equation 2.

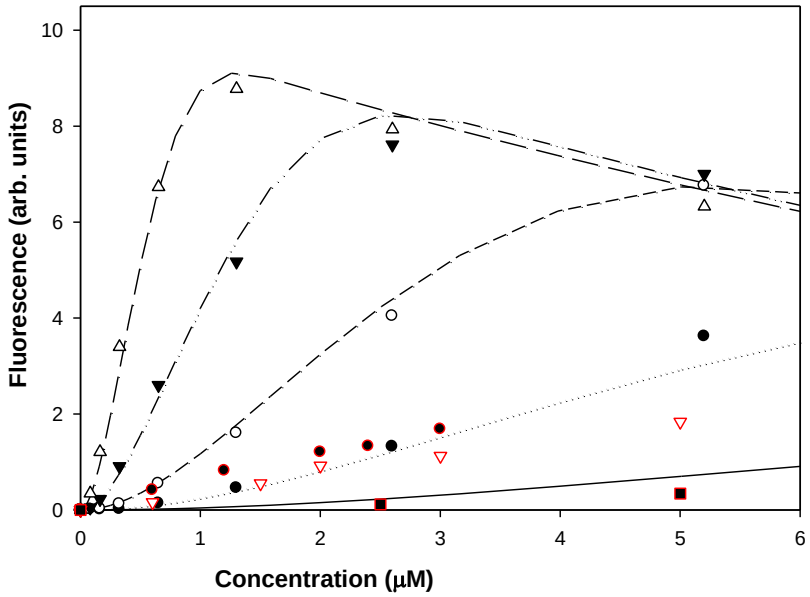


Figure 5: Simulated generation of fluorescence based on the rate equation model of Equations 2-4, for dendrimer generations 3-7 (lines). Also shown are the experimental

data for PAMAM dendrimers G4(●), G5(○), G6(▼), G7(Δ), and PPI dendrimers G2(■), G3(▽), G4(●).

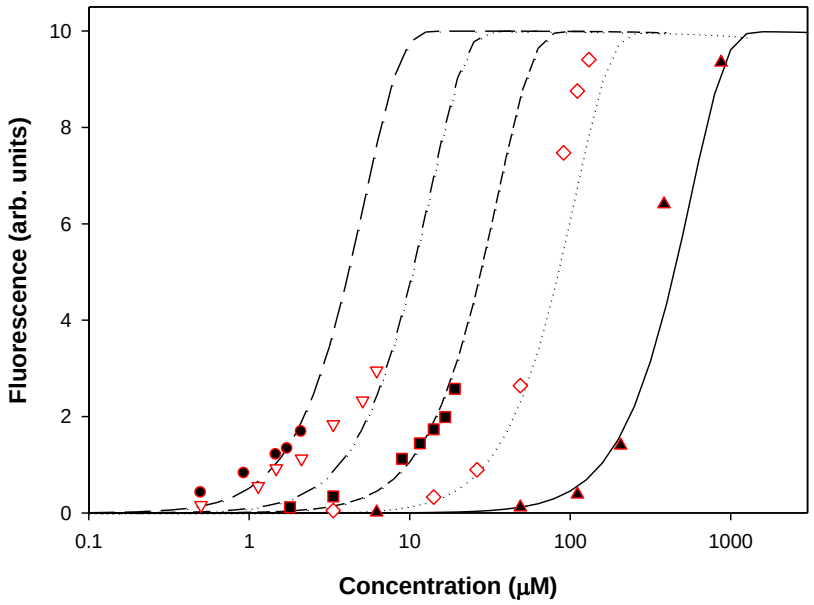


Figure 6: Simulated generation of fluorescence based on the rate equation model of Equations 2-4, for PPI dendrimer generations 0-4 (lines). Also shown are the experimental data for PPI dendrimers G4(●), G3(▽), G2(■), G1(◇), G0(▲)

Critically, the model confirms that the rate of increase of the dye fluorescence is explicitly related to the number of surface amino groups of the dendrimer species. Notably, the same equations and fit parameters for PAMAM give an acceptable simulation of the responses for the higher order generations of PPI (G2-G4). However, the simulations deviate from the observed experimental data substantially for lower PPI generations. A better reproduction of the generation dependent behaviour of the PPI series is achievable by utilising the same Equations 2-4, with a slightly increased initial

reaction rate and a substantial reduction of the rate of quenching of the fluorescence in the presence of the PPI dendrimers (see supplementary material; Table S1).

The simulation of the reaction based on a rate equation model supports the assumption that the acellular reaction of Figure 1, catalysed by the MAO-A enzyme, is further promoted by the presence of the polymeric dendrimers, and that the generation of $H_2O_2$ and subsequently Carboxy-$H_2$DCFDA fluorescence is quantitatively related to the number of surface amino groups and therefore surface reactivity of the dendrimer nanoparticles. The saturation of the reaction at high concentrations is a result of quenching of the dye by the dendrimers, rather than a fouling of the catalytic action during the reaction process.

This observed relationship suggests that the assay may be used to link the acellular NP reactivity and the *in vitro* toxic response, and this is supported by the correlations observed between ARR and $1/EC_{50}$ for each series (figure 4). However, the observed correlations are different for each series. PAMAM and PPI are related polymeric dendrimer series whose branches terminate in primary amino groups. PAMAM dendrimers contain a 2-carbon ethylenediamine core, whereas PPI contains a 4 carbon diaminobutane core.(*Images available at: symo-chem.nl, 2015 & dendritech.com, 2015*)[19,20] Although it may be assumed that their surface reactivity is determined by the number of surface amino groups and thus equivalent generations have similar reactivity, the PAMAM dendrimers are larger in diameter than the PPI series, even though PPI have a larger core.[37] In terms of the simulated responses, the experimental data can be well reproduced with almost identical reaction rates, indicating a similar reactivity of the dendrimers with equivalent $N_{amg}$, although there is a slight difference in

$k_{12}$ for each dendrimer series and a substantial difference in quenching rate, $k_q$. The somewhat different reactivity of PPI and PAMAM dendrimers may be due to conformation change of PPI dendrimers causing the branches to fold-in, rendering the surface groups inactive.[38]

*Khalid et al. (2015)* have demonstrated that for both PAMAM and PPI dendrimers, once internalised in the cells, the early stage ROS is the primary source of the cytotoxic response after 24hrs, and that for each dendrimer series, a similar degree of early stage oxidative stress results in a similar degree of cytotoxicity.[27] In the models of *Mukherjee and Byrne (2013)*[10], and *Maher et al. (2014)*[9], the simulated uptake of PAMAM dendrimers was seen to be generation (or size) dependent, and, translating the model to the PPI series, the observed higher levels of intracellular ROS generation and toxic response are consistent with a higher rate of internalisation of the PPI G3 and G4 dendrimers, which are, as already mentioned, substantially smaller in diameter than their PAMAM counterparts, according to literature values.[37] Therefore, although for both homologous dendrimer series, the ARR is well correlated with the previously determined generation dependent cytotoxicity, indicating its potential as a predictive screening tool for toxicity, it is clear that the structural dependence of the cytotoxic response is not only determined by the surface reactivity and that size dependent cellular uptake rates and mechanisms should also be considered. In this context, it is noteworthy that this assay was also used to evaluate the acellular reactivity of polystyrene nanoparticles (PSNP), with diameter of 50nm and amine modified surface coatings. While these particles do give $EC_{50}$ values comparable to those of PAMAM and PPI dendrimers (in the HaCaT cell lines tested), the acellular data showed little to no reactivity, which may point to different

modes of cellular toxicity. However, data on the extent of surface functionalisation of the PSNP's was unavailable and so direct comparison of the number of surface amino groups was impossible.

Other enzymes such as NADPH oxidase (which has been implicated in the build up of ROS upon nanoparticle uptake[39,40]) could have been used. In living cells, nanoparticles are taken up into endosomes via the process of endocytosis and shortly afterwards, an initial increase of ROS is observed. This initial ROS increase is thought to be caused by NADPH Oxidase; an enzyme which is present in nearly all cell types. It produces superoxide anions ($O_2^-$) via the transfer of an electron from NADPH, via FAD, to oxygen ($O_2$). The resulting ($O_2^-$) is then rapidly dismutated to hydrogen peroxide ($H_2O_2$). This process may be facilitated by the v-ATPase proton pump mechanism. It is reported that the unsaturated surface amino groups sequester protons that are supplied by the v-ATPase (proton pump).[29] This process keeps the pump functioning and leads to the retention of one $Cl^-$ ion and one water molecule per proton.

However, MAO was used in this study as it has several advantages. The reaction is relatively simple and the FAD co-factor for the enzyme was already bound in the as-supplied product. Furthermore, NADPH oxidase produces super oxide ($O_2^-$) as an ROS, which would not be directly measurable via Carboxy-$H_2$DCFDA, and to use another dye would deviate from the intracellular data used for comparison.

In summary, while the assay shows potential for the development of experimental systems which can quantify NP reactivity and therefore toxicity acellularly, additional testing is required. The results from this assay, to date, have only been compared to the cytotoxicity of single cell line (HaCaT) and a more comprehensive set of comparisons

with toxicological data from various cell lines will be essential to validate the accuracy and applicability of the assay. The PAMAM and PPI dendrimers have a well defined structure and elicit well defined acellular responses. However, it would be necessary to test the assay system with a vast range of different classes of nanoparticles, notably to correlate the differing trends of correlation of ARR with toxicity for differing nanoparticle sizes and cellular uptake rates.

## Conclusion

The need for rapid and cost effective pre-screening protocols of the toxicological response of the vast array of emerging nanoparticle types is apparent and the emerging consensus on the paradigm of oxidative stress by generation of intracellular reactive oxygen species as a primary source of the toxic response suggests the development of acellular assays to screen for nanoparticle surface reactivity. In the quantitative validation of such assays, the use of homologous series of polymeric dendrimer nanoparticles in which the physico-chemical properties are precisely and systematically variable is invaluable.

This study has explored the potential of a MAO-A enzyme based assay, which generates the ROS $H_2O_2$, quantified by the conversion of the Carboxy-$H_2$DCFDA dye to its fluorescent form. The assay response is well correlated with nanoparticle dose and reactivity over a range of doses, for two different dendrimer series, independent of structure. For each dendrimer series, the assay response correlates well with the experimentally observed physico-chemical dependences of the cytotoxicological response. However, it is observed that the acellular assay/cytotoxicity correlations for the

different dendrimer series are significantly different; indicating that the intermediate steps of cellular uptake rates must be considered in the development of a more universal acellular screening solution.

**Acknowledgements**

This work was conducted in part under the framework of the INSPIRE programme, funded by the Irish Government's Programme for Research in Third Level Institutions, Cycle 4, National Development Plan 2007-2013, supported by the European Union Structural Fund. M Maher is funded through the DIT Fiosraigh President's Award for Research Excellence 2010.

**Funding Sources**

This research was supported in part by the Integrated NanoScience Platform, Ireland (INSPIRE), funded under the Higher Education Authority PRTLI (Programme for Research in Third Level Institutions) Cycles 4 and 5, co-funded by the Irish Government and the European Union Structural fund. M Maher is funded through the DIT Fiosraigh President's Award for Research Excellence 2010

**Declaration of interest**

The authors declare no conflict of interest related to the work presented in this manuscript.

## References

1: Project on Emerging Nanotechnologies (PEN) **2015**, http://www.nanotechproject.org/

2: De Jong, W. H. and Borm, P.J.A. Drug delivery and nanoparticles: Applications and hazards. *Int. J. Nanomed.* **2008**, 3, 133–149

3: Jain, K.K., P. Gupta, U. and Jain, N.K. Dendrimer toxicity: Let's meet the challenge. *Int. J. Pharm.* **2010**, 394, 122–142

4: Kroll, A., Pillukat, M.H., Hahn, D. and Schnekenburger, J. Current *in vitro* methods in nanoparticle risk assessment: Limitations and challenges. *Int. J. Pharm. Biopharm.* **2009**, 72, 370-377

5: Oomen, A., Bos, P., Fernandes, T., Hund-Rinke, K., Boraschi, D., Byrne, H.J., Aschberger, K., Gottardo, S., von der Kammer, F., Kühnel, D. *et al*. Concern-driven integrated toxicity testing strategies for nanomaterials - Report of the NanoSafety Cluster Working Group 10, *NanoTox.* **2014**, 8, 334-338

6: Meng, H., Xia, T., George, S. and Nel, A.E. A Predictive Toxicological Paradigm for the Safety Assessment of Nanomaterials, *ACS Nano* **2009**, 3, 1620-1627

7: Clark, K.A., White, R.H. and Silbergeld, E. K. Predictive models for nanotoxicology: Current challenges and future opportunities. *Regul. Toxicol. Pharm.* **2011**, 59, 361-512

8: Organisation for Economic Co-Operation and Development (OECD): Guidance Document On Developing and Assessing Adverse Outcome Pathways, *OECD*, ENV/JM/MONO(2013)6, **2013**.

9: Maher, M.A., Naha, P.C., Mukerjee, S.P. and Byrne, H.J. Numerical simulations of in vitro nanoparticle toxicity – the case of Poly(amido amine) dendrimers. *Toxicol. In Vitro* **2014**, 28, 1449-1460

10: Mukherjee S.P. and Byrne, H.J. Polyamidoamine Dendrimer Nanoparticle Cytotoxicity, Oxidative Stress, Caspase Activation and Infammatory Response: Experimental Observation and Numerical Simulation. *Nanomedicine: Nanotechnology, Biology, and Medicine* **2013**, 9, 202-211

11: Organisation for Economic Co-Operation and Development (OECD): Guidance Document on the Validation of (Quantative) Structure Activity Relationships [(Q)SAR] Models, *OECD*, ENV/JM/MONO(2007)2, **2007**

12: Xia, T., Kovochich, M., Brant, J., Hotze, M., Sempf, J., Oberley, T., Sioutas, C., Yeh, J.I., Wiesner, M.R. and Nel, A.E. Comparison of the Abilities of Ambient and Manufactured Nanoparticles To Induce Cellular Toxicity According to an Oxidative Stress Paradigm. *Nano Lett.* **2006**, 6(8), 1794-1807

13: Wolinsky, J.B. & Grinstaff, M.W. Therapeutic and diagnostic applications of dendrimers for cancer treatment. *Adv. Drug Delivery Rev.* **2008**, 60(9), 1037–1055

14: Mukherjee, S.P., Davoren, M. and Byrne, H.J. In vitro mammalian cytotoxicological study of PAMAM dendrimers -towards quantitative structure activity relationships. *Toxicol. in Vitro* **2010**, 24,169-177 – A

15: Mukherjee, S.P., Lyng, F.M., Garcia, A., Davoren, M. and Byrne H.J. Mechanistic studies of in vitro cytotoxicity of Poly(amidoamine) dendrimers in mammalian cells. *Toxicol. Appl. Pharmacol.* **2010**, 248, 259–268 – B

16: Naha, P.C., Davoren, M., Lyng, F.M. and Byrne, H.J. Reactive Oxygen Species (ROS) induced cytokine production and cytotoxicity of PAMAM dendrimers in J774A.1 cells. *Toxicol. Appl. Pharmacol.* **2010**, 246, 91-99

17: Naha, P.C., Davoren, M., Casey, A. and Byrne, H.J. An Ecotoxicological Study of Poly (amidoamine) Dendrimers –Towards Quantitative Structure Activity Relationships. *Environ. Sci. Technol.* **2009**, 43, 6864-6869

18: Naha P.C. and Byrne, H.J. Generation of Intracellular Reactive Oxygen Species and Genotoxicity effect to Exposure of Nanosized Polyamidoamine (PAMAM) dendrimers in PLHC-1 cells in vitro. *Aquat. Toxicol.* **2013**, 132– 133, 61– 72

19: SyMO-Chem, **2015** (available at: http://www.symo-chem.nl/)

20: Dendritech, **2015** (Available at: http://www.dendritech.com/pamam.html)

21: Monteiro-Riviere, N. A., Nemanich, R. J., Inman, A. O., Wang, Y.Y. and Riviere, J. E. Penetration of Intact Skin by Quantum Dots with Diverse Physicochemical Properties. *Toxicol. Lett.* **2005**, 155, 377-384

22: Kesharwani, P., Jain, K. and Jain, N.K. Dendrimer as nanocarrier for drug delivery. *Prog. Polym. Sci.* **2014**, 39, 268– 307

23: Nanjwade, B.K., Bechra, H.M., Derkar, G.K., Manvi, F.V. and Nanjwade, V.K. Dendrimers: Emerging polymers for drug-delivery systems. *Eur. J. Pharm. Sci.* **2009**, 38, 185-196

24: Eichman, J.D., Bielinska, A.U., Kukowska-Latallo, J.F. and Baker, J.R.Jr. The use of PAMAM dendrimers in the efficient transfer of genetic material into cells. *J. Pharm. Sci. Technol.* **2000**, 3, 233-245

25: Duncan, R. and Izzo, L. Dendrimer biocompatibility and toxicity. *Adv. Drug. Deliv. Rev*. **2005**, 57, 2215– 2237

26: Akhtar, S., Al-Zaid, B., El-Hashim, A.Z., Chandrasekhar, B., Attur, S., Yousif, M.H.M. and Benter, I.F. Cationic Polyamidoamine Dendrimers as Modulators of EGFR Signaling *In Vitro and In Vivo*. PLoS ONE, **2015**, 10, doi:10.1371/journal.pone.0132215

27: Khalid, H., Byrne, M., Heise, A., Mukherjee, S.P., O'Neill, L. and Byrne, H.J. Structural dependence of the In vitro cytotoxicity, oxidative stress and uptake mechanisms of Poly(propylene imine) dendritic nanoparticles. *J. Appl. Toxicol.* **2015**, *Accepted for publication: 24-10-2015.*

28: Commission Recommendation of 18 October 2011 on the definition of nanomaterials. *Official Journal of the European Union*, **2011**, 2011/696/EU, L275/38 – L275/40.

29: Nel, A.E., Mädler, L., Velegol, D., Xia, T., Hoek, E.M.V., Somasundaran, P., Klaessig, F., Castranova, V. and Thompson, M. Understanding biophysicochemical interactions at the nano–bio interface. *Nat. Mater.* **2009**, 8, 543 - 557

30: Shi, M., Kwon, H.S., Peng, Z., Elder, A. and Yang, H. Effects of surface chemistry on the generation of reactive oxygen species by copper nanoparticles. *ACS Nano* **2012**, 6(3), 2157-2164

31: Sigma-Aldrich, **2015**. (Available at: http://www.sigmaaldrich.com/catalog/product/sigma/m7316?lang=en&region=IE)

32: Kim, S.Y., Nishioka, M. & Taya, M. Promoted proliferation of an SOD-deficient mutant of Escherichia coli under oxidative stress induced by photoexcited TiO2. *FEMS Microbiol. Lett.* **2004**, 236, 109–114

33: Yeber, M.C., Rodriguez, J., Freer, J., Duran, N. & Mansilla, H.D. Photocatalytic degradation of cellulose bleaching effluent by supported TiO2 and ZnO. *Chemosphere* **2000**, 41, 1193–1197

34: Fubini, B. & Hubbard, A. Reactive oxygen species (ROS) and reactive nitrogen species (RNS) generation by silica in inflammation and fibrosis. *Free Radic. Biol. Med.* **2003**, 34, 1507–1516

35: Venkatachari, P., Hopke, P.K., Grover, B.D. & Eatough D.J. Measurement of Particle-Bound Reactive Oxygen Species in Rubidoux Aerosols. *J. Atmos. Chem.* **2005**, 50, 49–58

36: Setareh-biotech, **2015** (Available at: http://www.setarehbiotech.com/details.cfm?ProdID=158)

37: Crooks, R.M., Zhao, M., Sun, L., Chechik, V. & Yeung, L.K. Dendrimer-encapsulated metal nanoparticles: synthesis, characterization, and applications to catalysis. *Acc. Chem. Res.* **2001**, 34, 181-90

38: He, D. Studies of PPI Dendrimers – Structures, Properties and Potential Applications. MSc, Marshall University, Huntington, West Virginia **2002**

39: Dostert, C., Pétrilli, V., Van Bruggen, R., Steele, C., Mossman, B.T. and Tschopp, J. Innate Immune Activation Through Nalp3 Inflammasome Sensing of Asbestos and Silica. *Science* **2008**, 320, 674-677

40: Nabeshi, H., Yoshikawa, T., Matsuyama, K., Nakazato, Y., Tochigi, S., Kondoh, S., Hirai, T., Akase, T., Nagano, K., Abe, Y., Yoshioka, Y., Kamada, H., Itoh, N., Tsunoda, S. and Tsutsumi, Y. Amorphous nanosilica induce endocytosis-dependent ROS generation and DNA damage in human keratinocytes. *Part. Fibre Toxicol.* **2011**, 8(1), 10 pages.